

# The Synthesis of Zinc Oxide Nanostructures as an Effective Photoanode for the applications of Dye Sensitized Solar Cells: ZnO Nanoflower, ZnO Nanorod, ZnO Nanoball

Jeevya Manickavasagar<sup>1</sup>, Amira Saryati Ameruddin<sup>1\*</sup>

<sup>1</sup> Department of Physics and Chemistry, Faculty of Applied Sciences and Technology, UTHM Kampus Cawangan Pagoh, Hab Pendidikan Tinggi Pagoh, KM 1, Jalan Panchor, 84600 Pagoh, Muar, Johor, MALAYSIA

\*Corresponding Author: [amira@uthm.edu.my](mailto:amira@uthm.edu.my)

DOI: <https://doi.org/10.30880/ekst.2024.04.02.048>

## Article Info

Received: 27 December 2023

Accepted: 12 January 2024

Available online: 12 December 2024

## Keywords

Fire-Resistant Materials, Household Ingredients, Corn-Starch, Baking Soda, Pva Glue, Hygroscopic Nature, Thermal Conductivity, Insulator, Conductor, Fire Resistivity, Binding Agent, Combustion, Material Science, Moisture Absorption, Innovation, Safer Environments

## Abstract

The field of dye-sensitized solar cells (DSSCs) has garnered significant attention due to its potential as a clean and sustainable energy source. This research focuses on the synthesis of ZnO nanostructures to enhance the performance of DSSCs. Three distinct ZnO nanostructures are synthesized utilizing the hydrothermal method and precipitation, aiming to investigate their suitability as photoanodes for DSSCs. Zinc oxide (ZnO) is a promising material for dye-sensitized solar cells (DSSCs), but its efficiency has not peaked. This study focuses on crucial factors like ZnO nanostructure type and morphology, exploring their impact on light absorption, dye sensitization, and charge carrier transportation. Understanding these factors could enhance ZnO-based DSSC efficiency, advancing solar energy conversion technology. The primary objective of this project is threefold, that is. The hydrothermal method, conducted in an autoclave, is employed for the synthesis of ZnO nanostructures, ensuring precise control over their morphological characteristics. Doctor blade method is employed as coating method on the FTO glass the fabricated ZnO nanostructured photoanodes are comprehensively analyzed using FESEM, UV-vis spectroscopy, and 4- point probe measurements to assess their surface morphology, optical properties, and electrical characteristics, respectively. The results reveal crucial insights into the effectiveness of ZnO nanostructured photoanodes for DSSCs. The synthesized nanostructures exhibit distinct morphologies such as nanoflower, nanorods and nanoballs, and optical characteristics, providing a basis for understanding their potential in enhancing the overall efficiency of DSSCs. This research contributes to the ongoing efforts in advancing renewable energy technologies by providing a detailed analysis of ZnO nanostructures as promising photoanode materials for DSSCs.

## 1. Introduction

Utilizing solar energy to produce power has been pointed to be one of the most promising answers to the world's energy crisis. Solar energy can meet all the world's energy needs and is abundant, limitless, and ecologically friendly [1]. Continuous thermonuclear fusion in the sun produces energy followed by emitting significant electromagnetic radiation and provides Earth's surface with more energy in an hour than the entire world consumes in an entire year [2]. This idea suggests that solar energy conversion is a viable option for supplying the world's energy need in the future. DSSC is exceptionally attractive due to its advantages such as simple fabrication, flexibility, operational simplicity, and employment of low-cost materials that are abundant in nature [3]. Schematically, a DSSC is made up of conducting substrates (FTO/ITO/conducting flexible sheets), semiconductor active layer (ZnO photoanode layer), a photosensitizer (dye), a redox mediator (electrolyte) and a counter electrode. The operation of DSSC is in some measure homologous to the photosynthesis phenomena that naturally occurs in plants. In DSSC, the light harvesting mechanism is done by the photosensitizer (dye). They can be in organic or non-organic form.

Whereas, in photosynthesis, the dye is the green, light harvesting pigment, called chlorophyll. In addition to replace oxidized dihydro-nicotinamide adenine dinucleotide phosphate (NADPH), the semiconductor created using nanostructured materials with a large band gap, such as ZnO, also serves as an electron acceptor (like CO<sub>2</sub>) in photosynthesis by absorbing electrons in its conduction band. The I-/I<sup>-3</sup> electrolyte replaces water [4]. Adding to this, the working principle of a DSSC is based on four steps that is light absorption, electron injection, transportation of carrier and collection of current. Predominantly, DSSC generates electrical energy by incident solar radiation without a permanent chemical transformation [5]. One of the most important components of the DSSC is the photoanode.

Zinc oxide (ZnO) is a promising material for dye-sensitized solar cells (DSSCs), but its efficiency has not peaked. This study focuses on crucial factors such as ZnO nanostructure type and morphology, exploring their impact on light absorption, dye sensitization, and charge carrier transportation. Understanding these factors could enhance ZnO-based DSSC efficiency, advancing solar energy conversion technology.

### 1.1 Semiconductor Oxide Photoanode

The working electrode that has been coated with semiconductor materials makes up the photoanode [6]. It is often coated with semiconductor wide bandgap metal oxide deposited on the TCO substrate. The photoanode is a crucial part of the DSSC because it serves as both a charge transport medium and a matrix for dye adsorption. This allows for the collection and movement of electrons. A high surface area for optimum dye loading, a wide energy direct bandgap to minimize incident photon loss on dye, high electron mobility to promote electron transport, and high transparency are all crucial features of an effective photoanode. Diffusion is a key electron transport pathway in DSSC [7]. The excited dye injects its electron into the semiconducting material when it is excited by incident photons. For everything to proceed effectively, it is also necessary to optimize the surface morphology [8]. The process of converting energy depends heavily on electron transport. Therefore, following the efficiency of the photoanode, the kind of nanostructure of the semiconducting material determines, mostly through surface morphology, the effectiveness of electron transit [9].

### 1.2 Zinc Oxide as a semiconducting oxide material for photoanodes.

A semiconductor with a wide band gap is zinc oxide (ZnO). The most noteworthy advantage of ZnO is its extraordinarily high electron mobility, which is more than an order of magnitude higher than that of anatase TiO<sub>2</sub>. High electron mobility is essential for facilitating electron transport since it reduces the recombination loss [5]. Zinc oxide (ZnO) can be synthesized into a broad variety of nanostructures, each of which can have unique properties for photo-catalysis, due to its anisotropic growth and ease of crystallization [10]. ZnO is another useful semiconductor material for photoanodes because to its high electron mobility (155 cm<sup>2</sup> V<sup>-1</sup> S<sup>-1</sup>) and large free excitation binding energy (60 meV) [11]. Interestingly, the ZnO crystal structure allows for several morphological changes. The various nanostructure forms can improve the energy conversion efficiency of DSSCs and electron mobility [12]. ZnO nanostructures have been created so far in a wide variety of morphologies, including nanotubes, nanoparticles, nanobelts, nanoclusters, nanowires, nanoflowers, and nano colloids. The one- to two-dimensional nanostructures of the ZnO photo-anode provide a discernible advantage in electron transport [13]. By permitting photoexcited electrons in the photo-anode to move in a unidirectional fashion rather than in zigzag or random patterns, they facilitate the rapid injection of electrons from dye into the semiconductor oxide layer. The goal of this study is to create three different kinds of ZnO nanostructures—ZnO nanorods, ZnO nanoflowers, and ZnO nanoparticles—as variables for the semiconducting material used in the photoanode. By means of these different precursors, reaction time and temperature are used to hydrothermal synthesis of these nanostructures.

## 2. Experimental Section

### 2.1 Materials

All the chemicals were purchased from Sigma Aldrich. Zinc nitrate hexahydrate ( $\text{Zn}(\text{NO}_3)_2 \cdot 6\text{H}_2\text{O}$ ), hexamethylenetetramine (HMTA), sodium hydroxide (NaOH) pellets, Polyvinylpyrrolidone (PVP), Zinc acetate dihydrate ( $\text{Zn}(\text{CH}_3\text{COO})_2 \cdot 2\text{H}_2\text{O}$ ), citric acid monohydrate ( $\text{C}_6\text{H}_8\text{O}_7 \cdot \text{H}_2\text{O}$ ). Materials used for paste: Triton X-100, and nitric acid, ethanol.

### 2.2 Synthesis of ZnO Nanoflower

All the chemicals were used without further purification and were of analytical grade. ZnO nanoflowers were fabricated by hydrothermal technique. 67 ml deionized water, 13 ml ethanol, and 0.35 g of zinc acetate dihydrate ( $\text{Zn}(\text{CH}_3\text{COO})_2 \cdot 2\text{H}_2\text{O}$ ) and 0.24 g of citric acid monohydrate ( $\text{C}_6\text{H}_8\text{O}_7 \cdot \text{H}_2\text{O}$ ) were dissolved while being vigorously stirred during the usual synthesis. After that, the solution was stirred and 10 M NaOH solution was added till the pH reached 13. The homogeneous solution was then completely mixed and then put into a Teflon-lined autoclave with a capacity of 100 ml. After that, the autoclave was heated for 17 hours at a steady 150 °C. The autoclave was let to naturally cool down to ambient temperature. The white products were then recovered by centrifugation, extensively cleaned with ethanol, and deionized water multiple times, and dried for 12 hours at 80 °C.

### 2.3 Synthesis of ZnO Nanorod

Separate precursor solutions of 0.1 M  $\text{Zn}(\text{NO}_3)_2 \cdot 6\text{H}_2\text{O}$  and 0.1 M HMTA were made for a duration of 30 minutes with continuous stirring. PVP (50 mg) surfactant solution was made in 40 ml of water. After that, it was added to the salt solution and stirred continuously for 15 minutes. The previously produced solution was mixed with the HMTA solution dropwise for 1 hour at room temperature. The resultant cloudy mixture was then transferred into a Teflon-lined autoclave. For 16 hours, the autoclave was kept in an oven set at 100°C. Following the prescribed duration of time, the white precipitates were cleaned with ethanol and water before being dried for 6 hours at 60°C in drying oven.

### 2.4 Synthesis of ZnO Nanoballs

The 0.8 M NaOH solution was mixed with 0.2 M zinc nitrate hexahydrate solution. The final mixture was continuously stirred before being put in a 100 ml Teflon beaker and placed into a stainless-steel autoclave. Autoclave held for four hours at 100 °C. Filter paper was used to collect the residue when the reaction was finished. The sample was repeatedly cleaned with ethanol and DI water before being dried at 60 °C to produce a white powder that included ZnO nanoballs.

### 2.5 ZnO photoanode preparation

For 10 minutes, the FTO glass was cleaned in an ultrasonic bath containing ethanol, acetone, and DI water. An air blower was used to dry the glass after it had been cleaned. In a mortar, 1 gram of ZnO nanopowder was combined with 6 mL of ethanolic solution, which is a blend of DI water and ethanol. Subsequently, 0.5 mL of 0.1 M nitric acid was added as an additive to enhance the connectivity and homogeneity of the particles. This was followed by 0.5 mL of Triton X-100, which functions as a binder to inhibit ZnO particle congregation and enhance the ZnO film's contact with the glass substrate. A paste was formed by grinding the mixture. The doctor blade method was then used to apply the paste on the conductive side of the FTO glass. By using this technique, the active part of the glass substrate was left uncovered so that the ZnO paste could be deposited by applying scotch tape to its edges. The paste was applied and then uniformly spread throughout the substrate using a glass rod. The tapes were removed prior to the sintering process. All the FTO glasses coated by respective nanostructures (ZnO nanoflower, ZnO nanorod and ZnO nanoball) were sintered in a furnace for 1 hour at 450°C.

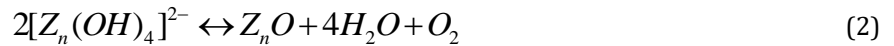
### 2.6 Characterization

COXEM EM30AX PLUS Model of Scanning Electron Microscope (SEM) was used to characterize the surface morphology of the nanostructures, The electrical characterization was done by Pro-4 Probing Station Model LUCAS LABS, Optical characterization was carried out using UV-Vis Spectrometer HITACHI U-3900H. The DEKTAK XT BRUKER model of Surface Profiler was used to measure the thickness of the ZnO nanostructure coating on the FTO glass.

### 3. Results and Discussion

#### 3.1 Morphological Characteristics

FESEM and SEM are used to examine the surface morphology of the ZnO nanostructures, as shown in Fig. 1. As shown in Fig. 1 (a and b), flower-like ZnO consisting of nanoparticles forms at 17 hours of reaction time. The flower-like shape was 1-2  $\mu\text{m}$  in size, with petals ranging from 100-350 nm. The petal surface roughness was ascribed to the aggregation of nanoparticles. There are numerous petals and pores in this unusual hierarchical flower-like structure, and these features will be crucial in enhancing electron transmission [14]. The hydrothermal process may involve the following chemical reactions:



It is commonly recognized that nucleation and crystal growth processes can be used to control the growth of ZnO, with nucleation taking place first and crystal growth following. At higher PH values, the nucleation rate is modest, and the crystal growth is relatively quick. The complex  $[\text{Zn}(\text{OH})_4]^{2-}$  can be readily associated with the surface at different sites of ZnO seeds because it has fewer nuclei and a greater number of growth units. It then grows along the corresponding axis into petal-like crystals that form flower-like structures. With exact control over the experimental parameters, including the kinds of precursors, the temperature and duration of stirring, the autoclave reaction time, and the heating temperature [16]. It is possible to successfully construct the well-defined, uniform nanorods with a high aspect ratio and increased surface area that are depicted in Fig. 1 (c and d).

The hydrothermal approach has advantages in terms of ease of use, scalability, and the capacity to precisely regulate the size and shape of ZnO nanostructures [15]. The resulting ZnO nanorods show a consistent distribution of diameter and length. Based on SEM pictures, the average length of the nanorods is between 700 and 900 nm. The length distribution shows that the intended nanorod length was achieved by a carefully regulated development procedure. In terms of diameter, the nanorods show a range of 90 to 150 nm. The distribution suggests a consistent nucleation and growth process during the hydrothermal synthesis. The variation in diameter can be attributed to the reaction kinetics and growth conditions within the autoclave. As for the third nanostructure, synthesized by the same hydrothermal method but different growth parameters, nanoballs are formed. All the nanoball samples were composed of large numbers of nanosheets. Before the formation of nanoball, the nanosheets were produced first. Then, due to the coulomb attraction of polar surface of zinc these nanosheets accumulated to form the nanoballs [16]. Importantly, the hydrothermal temperature, concentration of  $\text{Zn}^{2+}$  and  $\text{OH}^-$  played key role in the formation of nanoballs. First growth along the respective plane leading to the formation of ZnO nanosheets. Thickness of the nanosheets is also distressed by the hydrothermal temperature. To lower the surface energy, the nanosheets were collected in one location after they formed. The assembly serves as the nanoball's core. The hydrothermal temperature, which may be caused by Vander Waals forces—can have an impact on the angle between the nanosheets. In order to create a spherical ball-shaped nanostructure and lower the system's overall interface energy, several nanosheets are generated since spherical structures have lower surface tension and energy.

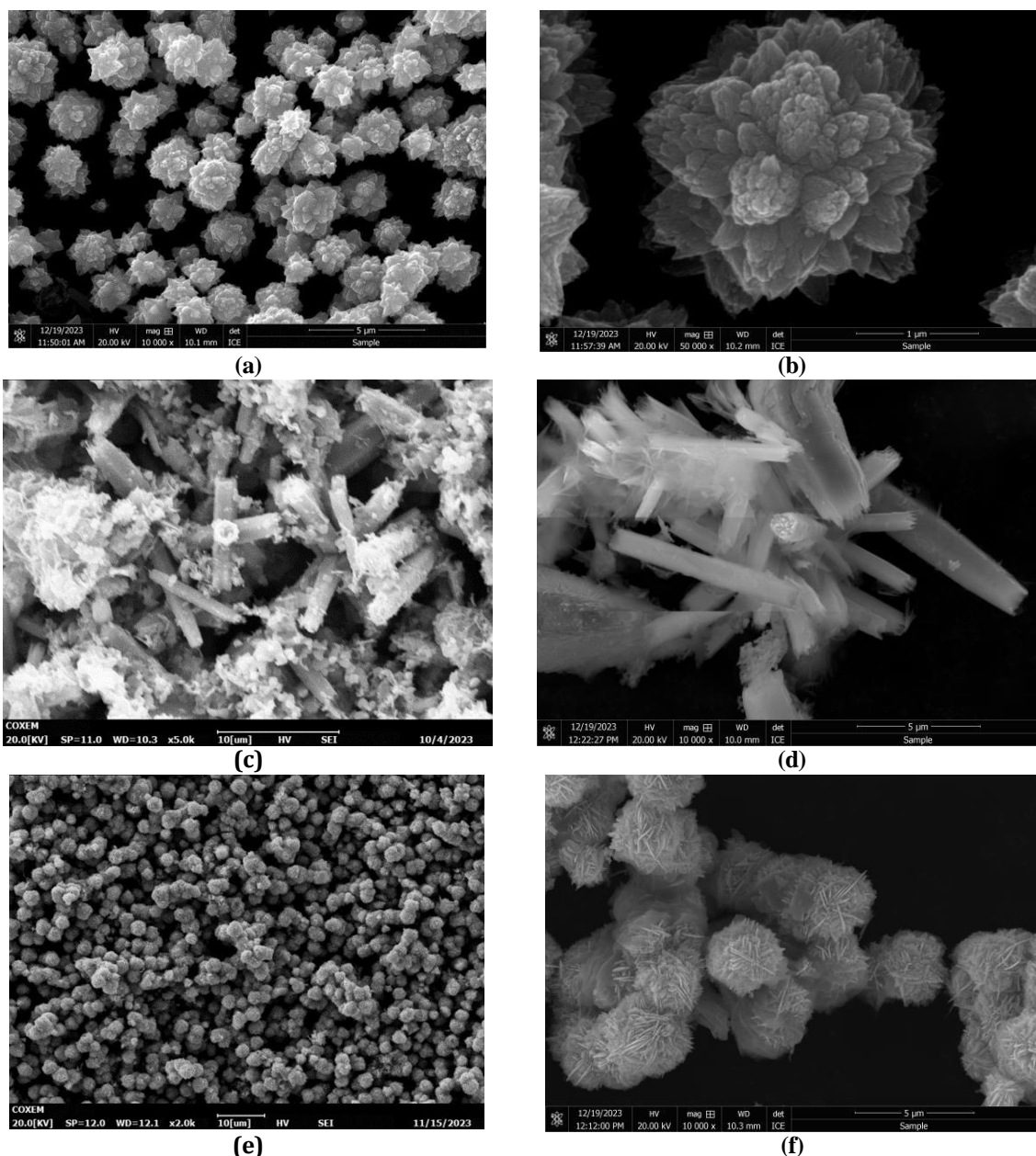


**Fig. 1** ZnO nanoflower (a) and (b), ZnO nanorods (c) and (d), ZnO nanoparticles (e) and (f).

### 3.2 Optical Characteristics

UV-Vis absorption spectroscopy was used to study the optical properties of the synthesized ZnO nanostructures. The main absorption peak at room temperature for ZnO nanoflower is at 245 nm. At 215 nm, for ZnO nanorod and a peak at 250 nm for ZnO nanoball. The optical transmittance and optical bandgap values of the ZnO nanostructured photoanode with all 3 nanostructures was also studied. This is illustrated in Fig. 2 (a) as wavelength versus transmittance and Fig. 2 (b) as the relationship between the wavelength and absorbance. The optical transmittance is calculated by using the equation 3 as below. A good photoanode will have a good transparency as more light should be transmitted to the dye that is adsorbed onto the semiconductor layer [17]. Since the dye acts as the electron pump by the dye's excitation, the pumped electron will be injected to the semiconductor material for electron transportation [18]. More light should be transmitted so that more electrons can be excited and hence the injected electrons will be higher. This will be contributed to higher current production in the DSSC, hence improving the efficiency [19]. Here, ZnO nanorod has the highest transmittance which is 98%. This might be due to the arrangement of ZnO nanorods on the photoanode. The vertical alignment of the nanorods might provide lesser surface area compared to other nanostructures as it does not capture higher number of photons. The nanoflower's transparency is good too since it has an average of 97% transmittance and nanoballs being the least with 92% transparency. The nanoflower has a higher surface area compared to nanorods since the branched and intricate structure of nanoflowers provides multiple surfaces,

edges, and crevices, contributing to an increased effective surface area. The bandgap energy of the ZnO nanostructures is calculated by the extrapolation of the linear portion of the graph between the function  $(\alpha hv)^2$  versus photon energy  $(hv)$  as shown in Fig. 3. The bandgap of nanoflower is 4.67 eV, ZnO nanorod is 5.34 eV and ZnO nanoball is 4.505 eV, noting that ZnO nanorod has the highest bandgap energy and ZnO nanoball has the lowest bandgap energy. The increase in the band gap of ZnO nanorods is attributed to their larger diameter compared to leaves in flowers. The effects may be explained by electron confinement, which is a phenomenon observed in nanomaterials, as well as changes in morphologies, defects, and grain size confinement [20]. To obtain the optical bandgap of a direct semiconductor, Tauc's model is applied as the following equation (4).

$$T = 10^{-A} \tag{3}$$

$$(\alpha hv) = A(hv - E_g)^2 \tag{4}$$

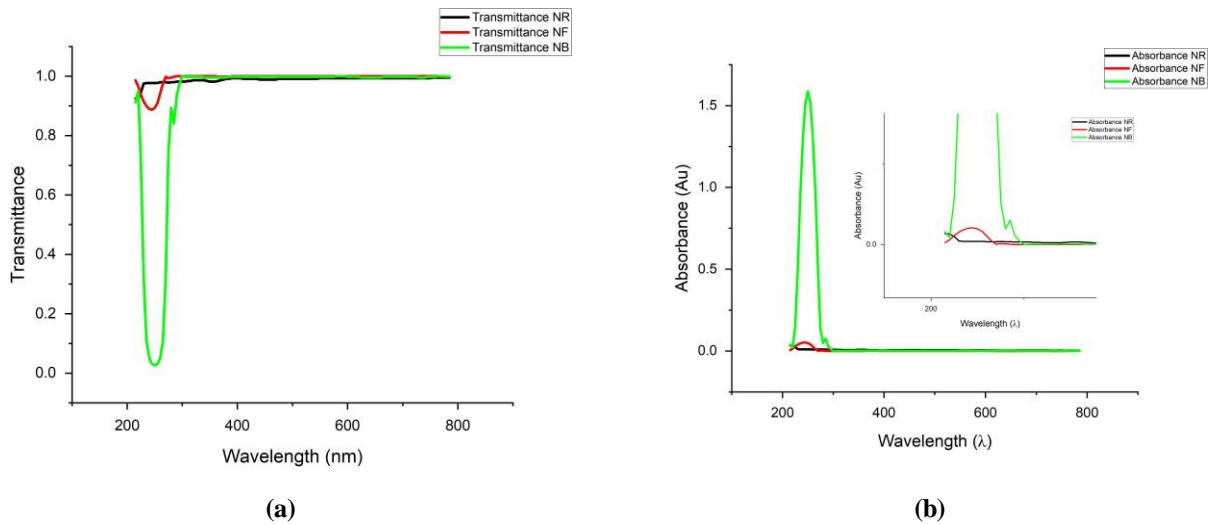


Fig. 2 Transmittance vs wavelength(a), Absorbance vs wavelength(b)

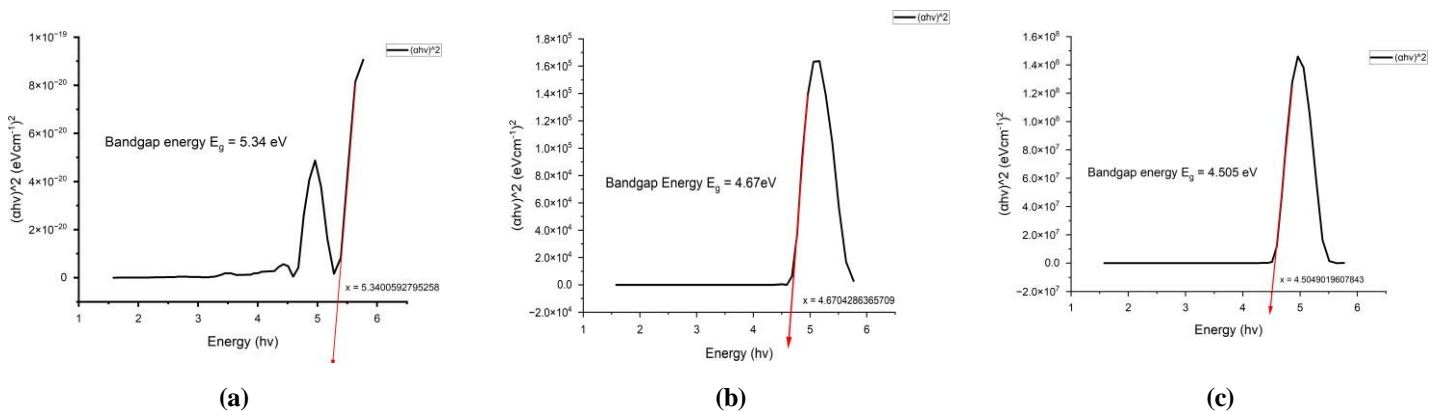


Fig. 3 Bandgap energy of ZnO Nanorod photoanode(a), ZnO Nanoflower photoanode(b), ZnO Nanoball Photoanode(c)

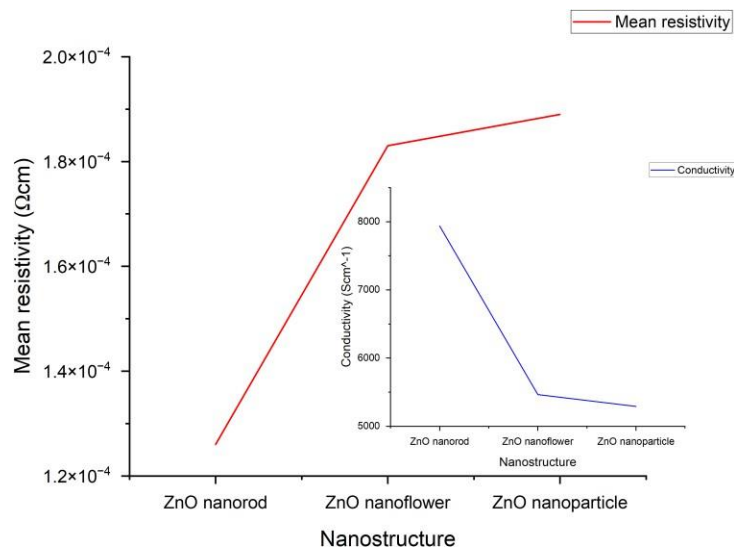
### 3.3 Electrical Characteristics

Table 1 shows the mean resistivity and conductivity which is the inverse of the ZnO nanostructured photoanodes. As we can see, the resistivity increases in the order of ZnO nanoflower, ZnO nanorod and ZnO nanoball. ZnO nanoflower has the least resistivity, hence highest conductivity among the 3 nanostructures. To explain this

phenomenon, higher carrier mobility means, the material has higher conductivity. The mobility of carriers which are affected by the crystalline and type of the nanostructure of the material was considered. Electrons from the excited dye are injected into the semiconducting oxide material in this case are the ZnO nanostructures. The injected electrons diffuse through the sintered nanostructure film, through a series of interparticle hopping steps, until they reach the collector electrode [21]. While electrons within individual particles are highly mobile, the numerous nanoparticle boundaries and dead ends in the disordered network limits the microscopic electron transportation [22]. ZnO nanoflowers provides a 3D structure and has a high surface area. The electrons will have a good diffusion network within these nanoflowers. The nano scaled petals will aid the electrons to diffuse efficiently and to reach the collector anode. In the ZnO nanorods, there are numerous boundaries and disordered networks, hence this will hinder the diffusivity of the electrons, hence limiting microscopic transportation. Also, since it's a disordered network the electrons will face many grain boundaries which in result will slow down its speed. For the ZnO nanoball, the nanostructure is packed with numerous nanosheets that are facing inwards that might be trapping agent of electrons. This might highly reduce the mobility/diffusivity of the electrons.

**Table 1** Mean resistivity and conductivity of ZnO nanostructures

Type of ZnO nanostructures	Mean Resistivity, $\rho$ ( $\Omega\text{cm}$ )	Conductivity, $\sigma$ ( $\text{Scm}^{-1}$ )
ZnO Nanoflower	$1.26 \times 10^{-4}$	7936
ZnO Nanorod	$1.83 \times 10^{-4}$	5464
ZnO Nanoball	$1.89 \times 10^{-4}$	5291



**Fig. 4** Mean resistivity and Conductivity of ZnO nanostructures

#### 4. Conclusion

Three kinds of nanostructures, ZnO nanoflowers, ZnO nanorods and ZnO nanoballs were synthesized by hydrothermal method to study the morphology dependent effective photoanode for DSSC properties. The different nanostructured ZnO materials synthesized by the hydrothermal method have been revealed to be promising material for the photoanode of DSSC. All three nanostructures have good transmittance for visible light, that is very much important for dye's light absorption and anti-degradation of the dye itself. Among the three, ZnO nanorods have good transmittance, most probably due to their vertical alignment. The electrical properties which are characterized by 4-point probe reveals that the ZnO has the highest electron conductivity, which will be very crucial for electron transportation and electron collection at the collector electrode and hence improving the efficiency of DSSC.

## Acknowledgement

I extend my gratitude to the Department of Physics and Chemistry, Universiti Tun Hussein Onn Malaysia (UTHM) for their unwavering support. Special thanks to the Nanophysics Lab team, Miss Maisarah, Dr. Amira Saryati, Mr. Izzat, Mr. Kamarul, Miss Fathin, Mr. Azman, and Mr. Azwadi from MiNT-SRC for their invaluable contributions to the successful completion of this project.

## Conflict of Interest

Authors declare that there is no conflict of interests regarding the publication of the paper.

## Author Contribution

*The authors confirm contribution to the paper as follows: **study conception and design, data collection, methodology, analysis and interpretation of results:** Jeevya Manickavasagar and Amira Saryati Ameruddin. All authors reviewed the results and approved the final version of the manuscript.*

## References

- [1] Hayat, M. B., Ali, D., Monyake, K. C., Alagha, L. & Ahmed, N. (2019). Solar energy—A look into power generation, challenges, and a solar-powered future. *International Journal of Energy Research*, 43(3), 1049–1067.
- [2] Vlachogianni, T. & Valavanidis, A. (2013). Energy and Environmental Impact on the Biosphere Energy Flow, Storage and Conversion in Human Civilization. *American Journal of Educational Research*, 1(3), 68–78.
- [3] Garcia Mayo, S. (2021). Dye-Sensitized Solar Cells (DSSCs): the future of consumer electronics?
- [4] Smestad, G. P. & Grätzel, M. (1998). Demonstrating electron transfer and nanotechnology: A natural dye-sensitized nanocrystalline energy converter. *Journal of Chemical Education*, 75(6), 752–756.
- [5] Vittal, R. & Ho, K. C. (2017). Zinc oxide based dye-sensitized solar cells: A review. In *Renewable and Sustainable Energy Reviews* (Vol. 70, pp. 920–935). Elsevier Ltd.
- [6] Abrol, S. A., Bhargava, C. & Sharma, P. K. (2021). Fabrication of DSSC using doctor blades method incorporating polymer electrolytes. *Materials Research Express*, 8(4).
- [7] Omar, A. & Abdullh, H. (2014). Electron transport analysis in zinc oxide-based dye-sensitized solar cells: A review. *Renewable and Sustainable Energy Reviews*, 31, 149–157. <http://dx.doi.org/10.1016/j.rser.2013.11.031>
- [8] Patel, N. A. & Patel, I. B. (n.d.). A Review of ZnO Nanoparticles Synthesized by Hydrothermal Method (Vol. 4). [www.ijariie.com](http://www.ijariie.com)
- [9] Dou, Y., Wu, F., Mao, C., Fang, L., Guo, S. & Zhou, M. (2015). Enhanced photovoltaic performance of ZnO nanorod-based dye-sensitized solar cells by using Ga doped ZnO seed layer. *Journal of Alloys and Compounds*, 633, 408–414.
- [10] Frederichi, D., Scaliante, M. H. N. O. & Bergamasco, R. (2021). Structured photocatalytic systems: photocatalytic coatings on low-cost structures for treatment of water contaminated with micropollutants—a short review. *Environmental Science and Pollution Research*, 28(19), 23610–23633.
- [11] Smith, Y. R., Crone, E. & Subramanian, V. (2013). A simple photocell to demonstrate solar energy using benign household ingredients. *Journal of Chemical Education*, 90(10), 1358–1361.
- [12] Andreani, L. C., Bozzola, A., Kowalczewski, P., Liscidini, M. & Redorici, L. (2019). Silicon solar cells: Toward the efficiency limits. *Advances in Physics: X*, 4(1). <https://doi.org/10.1080/23746149.2018.1548305>
- [13] Manabeng, M., Mwanemwa, B. S., Ocaya, R. O., Motaung, T. E. & Malevu, T. D. (2022). Influence of ZnO Nanostructure Morphologies on Perovskite Solar Cell Performance: A Review. *Processes*, 10(9), 1803. <https://doi.org/10.20944/preprints202208.0121.v1>
- [14] Agarwal, S., Rai, P., Gatell, E. N., Llobet, E., Güell, F., Kumar, M. & Awasthi, K. (2019). Gas sensing properties of ZnO nanostructures (flowers/rods) synthesized by hydrothermal method. *Sensors and Actuators, B: Chemical*, 292(February), 24–31. <https://doi.org/10.1016/j.snb.2019.04.083>
- [15] Djurisic, A. B., Xi, Y. Y., Hsu, Y. F. & Chan, W. K. (2007). Hydrothermal Synthesis of Nanostructures. 1, 121–128.
- [16] Sahu, K. & Kar, A. K. (2019). Morphological, optical, photocatalytic and electrochemical properties of hydrothermally grown ZnO nanoflowers with variation in hydrothermal temperature. *Materials Science in Semiconductor Processing*, 104(March), 104648. <https://doi.org/10.1016/j.mssp.2019.104648>
- [17] Guo, M., Chen, X. & Huang, H. (2014). *RSC Advances*. RSC Advances.
- [18] Hu, Y. H., Wei, W. & States, U. (2018). Dye-Sensitized Materials. In *Comprehensive Energy Systems* (Vol. 2). Elsevier Ltd. <https://doi.org/10.1016/B978-0-12-809597-3.00216-9>

- [19] Robertson, N. (2006). Optimizing dyes for dye-sensitized solar cells. In *Angewandte Chemie - International Edition* (Vol. 45, Issue 15, pp. 2338–2345).
- [20] Neikov, O. D. & Yefimov, N. A. (2019). Nanopowders. In *Handbook of Non-Ferrous Metal Powders* (2nd ed.). Elsevier Ltd. <https://doi.org/10.1016/B978-0-08-100543-9.00009-9>
- [21] Bisquert, J. (2007). Hopping Transport of Electrons in Dye-Sensitized Solar Cells. 17163–17168.
- [22] Kumar, R., Umar, A., Kumar, G., Nalwa, H. S., Kumar, A. & Akhtar, M. S. (2017). Zinc oxide nanostructure-based dye-sensitized solar cells. In *Journal of Materials Science* (Vol. 52, Issue 9, pp. 4743–4795). Springer New York LLC.